Experimental and Molecular Pathology 145 (2026) 105023

Contents lists available at ScienceDirect

Experimental and Molecular Pathology

journal homepage: www.elsevier.com/locate/yexmp

Antioxidant and neuroprotective effects of ubiquinol diacetate: Insights from SH-SY5Y cell line and *Caenorhabditis elegans* models of Parkinson's disease

Matteo Micucci [a,1], Michela Battistelli [a,1], Sabrina Burattini [a], Riham Osman [a], Francesco Onesimo [a], Michele Mari [a], Michele Retini [a], Ilaria Versari [b], Barbara Pagliarani [c], Andrea Tarozzi [c,d,*], Giovanni Zappia [e,f,*], Federico Gianfanti [a], Letizia Pruccoli [c]

[a] *Department of Biomolecular Sciences, University of Urbino Carlo Bo, Via Ca' Le Suore 2/4, 61029 Urbino, Italy*
[b] *Department of Biomedical and Neuromotor Sciences, University of Bologna, Via Massarenti 9, 40138 Bologna, Italy*
[c] *Department for Life Quality Studies, University of Bologna, Corso d'Augusto 237, 47921 Rimini, Italy*
[d] *Biostructures and Biosystems National Institute (INBB), Via dei Carpegna 19, 00165 Rome, Italy*
[e] *Department of Human Sciences and Promotion of the Quality of Life, University of San Raffaele, Roma, Italy*
[f] *Umolsystem Srl, Tecnopolo Roma-Castel Romano, Via di Castel Romano 100, 00128 Roma, Italy*

ARTICLE INFO

Keywords:
Antioxidant
Neuroprotection
Ubiquinol diacetate
Ubiquinone
Parkinson's disease

ABSTRACT

Parkinson's disease (PD) is a neurodegenerative disease characterized by the degeneration of dopaminergic neurons in the substantia nigra and the presence of misfolded α-synuclein in the brain. Mitochondrial dysfunction and oxidative stress are factors contributing to the death of these neurons. Coenzyme Q10 (CoQ10) serve as an antioxidant and cofactor for mitochondrial enzymes, and its deficiency can exacerbate neurodegenerative processes in PD. However, the clinical efficacy of CoQ10 is limited by its low bioavailability and instability. Ubiquinol diacetate (CoQ10 Ac), an esterified form of CoQ10, shows improved pharmacokinetic properties and potential as a prodrug, converting into the reduced antioxidant form of CoQ10 by esterases in the body. This study aimed to investigate the antioxidant and neuroprotective effects of CoQ10 Ac compared to CoQ10 in SH-SY5Y cell line and *Caenorhabditis elegans* models of PD. CoQ10 Ac showed higher antioxidant activity than CoQ10 at both extracellular and intracellular levels, particularly in the membrane and cytosolic compartments. It exhibited superior neuroprotection against 6-hydroxydopamine toxicity, showing a greater ability to reduce the activation of caspase-3 and PARP1 compared to CoQ10. Both compounds decreased the increased ratio of mitochondrial fission protein, DRP1, to fusion protein, OPA1, induced by 6-hydroxydopamine in SH-SY5Y cells, enhancing OPA1 levels and promoting antiapoptotic death. However, CoQ10 Ac was more effective than CoQ10 in preserving mitochondrial structural integrity and mass. Additionally, both compounds significantly inhibited the aggregation of α-synuclein induced by 6-hydroxydopamine. Furthermore, CoQ10 Ac showed stronger neuroprotective effects than CoQ10 in *C. elegans* models of PD. It demonstrated greater anti-aggregant activity in *C. elegans* expressing human α-synuclein, suggesting higher bioavailability. These findings highlight CoQ10 Ac as a promising prodrug candidate and support further investigation in *in vivo* PD models.

Abbreviations: PD, Parkinson's disease; α-syn, α-synuclein; ROS, reactive oxygen species; 6-OHDA, 6-hydroxydopamine; H_2O_2, hydrogen peroxide; ABTS, 2,2′-Azino-bis (3-ethylbenzothiazoline-6-sulfonic acid) diammonium salt; DPPH, 2,2-Diphenyl-1-picrylhydrazyl; DCFH-DA, 2′,7′-dichlorodihydrofluorescein diacetate; MTT, 3-(4,5-dimethyl-2-thiazolyl)-2,5-diphenyl-2H-tetrazolium bromide; NAO, 10-N-Nonyl Acridine Orange; MTG, MitoTracker™ Green; DMSO, dimethyl sulfoxide; HBSS, Hank's Balanced Salt Solution; TAA, total antioxidant activity; PBS, phosphate-buffered saline; AUF, Arbitrary Units of Fluorescence; RFU, Relative Fluorescence Units..

* Corresponding authors at: Department for Life Quality Studies, University of Bologna, Corso d'Augusto 237, 47921 Rimini, Italy (A. Tarozzi); Department of Human Sciences and Promotion of the Quality of Life, University of San Raffaele, Roma, Italy (G. Zappia).

E-mail addresses: matteo.micucci@uniurb.it (M. Micucci), michela.battistelli@uniurb.it (M. Battistelli), sabrina.burattini@uniurb.it (S. Burattini), r.osman@campus.uniurb.it (R. Osman), f.onesimo@campus.uniurb.it (F. Onesimo), michele.mari@uniurb.it (M. Mari), michele.retini@uniurb.it (M. Retini), ilaria.versari4@unibo.it (I. Versari), barbara.pagliarani2@unibo.it (B. Pagliarani), andrea.tarozzi@unibo.it (A. Tarozzi), giovanni.zappia@uniroma5.it (G. Zappia), federico.gianfanti@uniurb.it (F. Gianfanti), letizia.pruccoli2@unibo.it (L. Pruccoli).

[1] These authors contributed equally to this work.

https://doi.org/10.1016/j.yexmp.2026.105023
Received 23 July 2025; Received in revised form 19 December 2025; Accepted 5 January 2026
Available online 13 January 2026

1. Introduction

Parkinson's disease (PD) is a progressive neurodegenerative condition, hallmarked by the degeneration of dopaminergic neurons in the substantia nigra and the pathological aggregation of α-synuclein (α-syn) within Lewy bodies (Borsche et al., 2021; Raza et al., 2019). At the molecular level, mitochondrial dysfunction is a key factor in PD. In this regard, the inhibition of complex I and defects in the PINK1 and Parkin pathways result in the accumulation of damaged mitochondria and increased reactive oxygen species (ROS), resulting in oxidative stress (Moradi Vastegani et al., 2023). The oxidative stress is further intensified by dopamine metabolism, which amplifies neuronal damage. Protein homeostasis is disrupted by α-syn aggregation, which impairs mitochondrial function and lysosomal degradation pathways, accelerating neurodegeneration (Picca et al., 2021). This aggregation damages mitochondrial membranes, leading to impaired complex I activity and increased ROS production, creating a harmful feedback loop. Cellular dysfunction is further impaired by calcium dysregulation, neuroinflammation, and endoplasmic reticulum stress. Mutations in genes like SNCA, LRRK2, and POLG also worsen mitochondrial and lysosomal dysfunction, contributing to the progression of PD. These interconnected mechanisms emphasize the complexity of PD and its dependence on maintaining mitochondrial function and proteostasis (Borsche et al., 2021; Raza et al., 2019). Dietary supplements, also known as nutraceuticals, have health benefits for treating and preventing diseases like PD. They provide neuroprotection through mechanisms such as iron chelation, modulation of cell signaling, scavenging of superoxide radicals and ROS, and reducing inflammation (Sharma et al., 2025). Nutritional supplements like Coenzyme Q10, Lycopene, Resveratrol, and Omega-3 fatty acids provide neuroprotection through various mechanisms. They target issues such as alpha-synuclein misfolding, oxidative stress, mitochondrial dysfunction, and neuroinflammation. Recent studies also highlight that these emerging nutraceuticals, including vegetal extracts like *Acacia catechu*, *Castanea sativa*, *Olea europaea*, and *Hibiscus sabdariffa*, can share similar neuroprotective effects (Brizi et al., 2016; Chiaino et al., 2020, 2022; Santulli et al., 2017). By addressing these factors, these supplements may help slow disease progression and improve the quality of life for patients with PD. Coenzyme Q10 (also known as ubiquinone or CoQ10) is a vitamin-like, fat-soluble quinone that is widely distributed in the liver and the brain (Sharma et al., 2025). CoQ10 transfers electrons from complexes I and II to complex III of the mitochondrial respiratory chain. This process acts as an energy transfer mechanism in the electron transport chain, ultimately leading to the production of ATP, chemical energy. CoQ10 also acts as an antioxidant, protecting lipid-soluble cell membranes from oxidative damage by ROS. Its reduced form, ubiquinol (CoQ10H2), which must continually be regenerated from its oxidized form, CoQ10, to maintain its protective effects (Mantle and Dybring, 2020). CoQ10 deficiency in PD exacerbates neurodegenerative mechanisms, thereby justifying its supplementation as a promising therapeutic approach (Mischley et al., 2012). CoQ10 supplementation in PD patients has shown contrasting results (Müller et al., 2003; Negida et al., 2016; Seet et al., 2014; Storch, 2007; Yoritaka et al., 2015). This inconsistency stems from pharmacological issues, including an imbalance between its oxidized and reduced forms, which are crucial for mitochondrial function and antioxidant activity, and its poor bioavailability, which hinders it from reaching therapeutic concentrations in brain tissue. To overcome these limitations, several CoQ10 analogues, including Idebenone, Mitoquinone, Decylubiquinone, SkQ1, Short-Chain CoQ10, and EPI-743, have been investigated for their medical applications and antioxidant properties in preclinical and clinical settings (Ghosh et al., 2010; Suárez-Rivero et al., 2021; Ünal et al., 2020). Regarding strategies to improve the bioavailability of CoQ10, an early pharmacokinetic study in rats reported that administering different esterified forms of CoQ10H2 by dietary supplementation could increase the CoQ10 levels in blood (Turunen et al., 1999). In particular, CoQ10 levels were significantly greater in rats given the succinylated CoQ10 (40 %) and, particularly, the acetylated CoQ10 (70 %) than CoQ10. Recent pharmacokinetic studies have confirmed that the supplementation with CoQ10H2 diacetate (CoQ10 Ac) leads to a significant increase of both CoQ10 and CoQ10H2 levels in the plasma and liver of rats and guinea pigs (Passi et al., 2003). The results also indicate that after ingestion, CoQ10 Ac is easily hydrolyzed to CoQ10H2 by esterase enzymes in the duodenum and small intestine and, under this form, absorbed, at the same way it occurs with a-tocopheryl acetate. Several studies have described the neuroprotective effects of CoQ10, due to its ability to preserve mitochondrial activity, particularly the function of complex I and IV. This has been observed in various in vitro models of PD, including skin fibroblast from patients with PD and SH-SY5Y cells treated with rotenone (Millichap et al., 2024; Winkler-Stuck et al., 2004). In this regard, a more recent study has shown that CoQ10 Ac can also preserve mitochondrial ATP production, as well as cellular morphology and mitochondrial structures in HT22 hippocampal cells exposed to the neurotoxic effects of rotenone (Micucci et al., 2025). This highlights that mitochondrial dysfunction, particularly the inhibition of complex I, is a key mechanism of toxicity mediated by rotenone and is often associated with neurodegenerative diseases like PD. These findings warrant further investigation in experimental models of PD. In this study, we investigated the antioxidant and neuroprotective effects of CoQ10 and its acetylated form, CoQ10 Ac (Fig. 1), using the dopaminergic SH-SY5Y cell line and *Caenorhabditis elegans* Models of PD. In both models, we utilized the oxidant stressor 6-hydroxydopamine (6-OHDA) to induce features of the PD phenotype. 6-OHDA is found endogenously in human brain and urine samples, which lends additional credibility and evidence for its research use in preclinical models of PD (Andrew et al., 1993; Curtius et al., 1974; Galindo et al., 2014). Similarly to dopamine, 6-OHDA induces dopaminergic damage by generating semiquinones, which lead to ROS, such as hydrogen peroxide (H_2O_2) and hydroxyl radicals (Blum et al., 2001). In addition, 6-OHDA inhibits mitochondrial complex I and IV in the electron transport chain, leading to neuronal cell death (Thirugnanam and Santhakumar, 2022). Given that the aggregation and deposition of α-syn is a common pathological event in PD, we also evaluated the ability of CoQ10 and CoQ10 Ac to inhibit the α-syn aggregation induced by 6-OHDA. For this purpose, we utilized a novel green fluorescent SH-SY5Y cell line that was developed through stable transfection with TagGPF2-α-syn. In this regard, the anti-aggregant activity of CoQ10 and CoQ10 Ac was also evaluated in transgenic *C. elegans* that express YFP-fused human α-syn. While evaluating the antioxidant and neuroprotective profiles of CoQ10 and CoQ10 Ac in SH-SY5Y cells, we compared their activity at different treatment durations with the 6-OHDA. This comparison was made considering that the formation of the active form CoQ10H2 from CoQ10 and CoQ10 Ac in neuronal cells involves reducing enzymes and esterases, respectively.

2. Materials and methods

2.1. Chemicals and reagents

CoQ10, 2,2′-Azino-bis (3-ethylbenzothiazoline-6-sulfonic acid) diammonium salt (ABTS), 2,2-Diphenyl-1-picrylhydrazyl (DPPH), 2′,7′-dichlorodihydrofluorescein diacetate (DCFH-DA), 3-(4,5-dimethyl-2-thiazolyl)-2,5-diphenyl-2H-tetrazolium bromide (MTT), 6-OHDA and H_2O_2 were purchased from Sigma-Aldrich (Sigma-Aldrich, St. Louis,

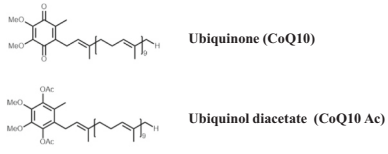

Fig. 1. Chemical structure of CoQ10 and CoQ10 Ac.

MO, USA). The diacetate CoQ10 derivative, CoQ10 Ac, was kindly provided by UMOLSYSTEM Srl (UMOLSYSTEM Srl, Rome, Italy). Trolox, 10-N-Nonyl Acridine Orange (NAO) and MitoTracker™ Green (MTG) were purchased from Thermo Fisher Scientific (Thermo Fisher Scientific, Waltham, MA, USA). All chemicals used in the experiments were of analytical grade.

2.2. Cell culture and preparation of compound solutions

The human neuroblastoma SH-SY5Y cells (catalog no. 94030304) were supplied by the European Collection of Authenticated Cell Cultures (ECACC, UK Health Security Agency, Porton Down, Salisbury, UK). TagGFP2-α-syn SH-SY5Y cells (catalog no. P30707) were purchased by Innoprot (Derio, Bizkaia, Spain). These two cell lines were routinely grown in Dulbecco's modified Eagle Medium supplemented with fetal bovine serum (10 %), L-glutamine (2 mM), penicillin (50 U/mL) and streptomycin (50 μg/mL) in a humidified incubator at 37 °C with 5 % CO_2. To perform experiments, we prepared stock solutions of CoQ10 and CoQ10 Ac in dimethyl sulfoxide (DMSO) at 2,5 mM. We diluted the stock solutions in a complete medium to achieve the required compound concentrations, ensuring that DMSO was below 0.1 %.

2.3. Determination of antioxidant activity

The antioxidant activity of the two compounds was assessed using DPPH and ABTS radicals. The DPPH assay was performed as previously described in (Pruccoli et al., 2020). Briefly, 150 μL of DPPH in ethanol (100 μM) was added to 50 μL of the compounds at different concentrations (2.5–40 μM) in a 96 well plate. After 30 min of incubation, the absorbance of the reaction solution was measured at 490 nm using the multilabel plate reader VICTOR™ X3 (PerkinElmer, Waltham, MA, USA). The ABTS assay was performed as previously described in (Pruccoli et al., 2024). Briefly, a 2 mM ABTS solution was mixed with potassium persulfate (7 mM) and kept in the dark at room temperature for 24 h to generate ABTS radicals. The ABTS solution was then diluted with phosphate-buffered saline (PBS) before being used to achieve an absorbance value of 0.70 at 734 nm. Subsequently, 1 mL of the diluted ABTS solution was added to 10 μL of the compounds at the concentration of 10 μM and the absorbance was measured after 1 min at 734 nm using the Jasco V-630Bio spectrophotometer (JASCO Europe S.r.l., Carpi, Mo, Italy). The antioxidant activity was expressed as the equivalent of micromoles of trolox per milliliter of compound solution.

2.4. Determination of total antioxidant activity in membrane and cytoplasm of SH-SY5Y cells

The Total Antioxidant Activity (TAA) of the membrane and cytoplasm of SH-SY5Y cells treated with CoQ10 or CoQ10 Ac was assessed using ABTS assay as previously described (Pruccoli et al., 2024). Briefly, cells were placed in 60 mm dishes at 2×10^6 cells per dish. After 24 h of incubation, cells were treated with CoQ10 and CoQ10 Ac at a concentration of 10 μM for 2 h at 37 °C in 5 % CO_2. After incubation, cells were washed three times with cold PBS and softly detached from the dish using a cell lifter. After collecting cells in 1 mL of PBS, they were centrifuged at 10,000 rpm for 10 min at 4 °C. The supernatant was removed and cells were again washed with 1 mL of PBS. This washing process was repeated twice, after which the pellet was reconstituted in 600 μL of lysis buffer containing Triton X-100 0.05 %. After homogenizing, cells were left to stand at 4 °C for 30 min. The mixture was centrifuged at 14,000 rpm for 15 min at 4 °C to extract the cytoplasmic fraction. The pellet was then dissolved in 400 μL of lysis buffer containing Triton X-100 1 % to obtain the membrane fraction. Membrane and cytoplasmic cell fractions were kept at −20 °C. Small amounts were taken out to determine the protein concentration using the Bradford method. The antioxidant activity of the two compounds was measured on membrane and cytoplasmic fractions using ABTS assay as described above. ABTS decolorization was compared to a standard curve of trolox, a water-soluble analogue of vitamin E, to calculate the TAA of membrane and cytoplasmic fractions. The trolox standard curve was prepared using concentrations ranging from 50 to 150 μM. TAA was expressed as the equivalent of micromoles of trolox per milligram of protein.

2.5. Determination of cellular antioxidant activity

The cellular antioxidant activity of the compounds was assessed in SH-SY5Y cells using the DCFH-DA assay, as previously described (Pruccoli et al., 2024). DCFH-DA is a fluorogenic probe for the detection of intracellular ROS. The cell-permeable DCFH-DA diffuses into cells and is deacetylated by cellular esterases to form 2′,7′-dichlorodihydrofluorescein. Then, in the presence of ROS, it is oxidized to 2′,7′-dichlorofluorescein, which is highly fluorescent. Briefly, cells were placed in a 96-well plate at 3×10^4 per well and incubated for 24 h. After incubation, the medium was removed and 100 μL of the fluorescent probe DCFH-DA in PBS (10 g/mL) was added to each well. The plate was then incubated for 30 min at room temperature. After incubation, the DCFH-DA solution was replaced with 100 μL of CoQ10 or CoQ10 Ac (5–10 μM) and H_2O_2 (200 μM). The plate was then incubated for another 30 min, after which the ROS formation was measured using the multitask plate reader VICTOR™ X3 (excitation at 485 nm and emission at 535 nm). Another set of SH-SY5Y cells was placed in a 96-well plate at 2×10^4 cells per well, incubated for 24 h and treated with CoQ10 or CoQ10 Ac (5–10 μM) for 24 h. After incubation, the treatment medium was discarded and 100 μL of DCFH-DA in PBS (10 g/mL) was added to each well. The plate was then incubated for 30 min at room temperature. After incubation, the DCFH-DA solution was replaced with 100 μL of H_2O_2 (200 μM). The ROS formation was measured after 30 min of incubation, as described above. Data were expressed as Arbitrary Units of Fluorescence (AUF).

2.6. Determination of neuroprotective activity against 6-OHDA in SH-SY5Y cells

The viability of cells was assessed using the MTT assay, as previously described [23]. Briefly, SH-SY5Y cells were placed in a 96-well plate, with 2×10^4 cells per well and incubated for 24 h. After incubation, cells were treated with various concentrations of CoQ10 or CoQ10 Ac (1.25–40 μM) for 24 h at 37 °C in 5 % CO_2. In parallel, the neuroprotective activity of CoQ10 and CoQ10 Ac against 6-OHDA-induced neurotoxicity was assessed in SH-SY5Y cells using the MTT assay. Cells were placed in a 96-well plate at 3×10^4 cells per well and incubated for 24 h. Then, cells were treated with CoQ10 or CoQ10 Ac (5–10 μM) and 6-OHDA (200 μM) for 2 h at 37 °C in 5 % CO_2. The treatment medium was subsequently replaced with MTT in HBSS (0.5 mg/mL), and then the plate was incubated for 2 h at 37 °C in 5 % CO_2. After washing the cells with HBSS, formazan crystals were solubilized in isopropanol. Finally, the amount of formazan was measured at 570 nm (reference filter 690 nm) using the multitask plate reader VICTOR™ X3 (PerkinElmer). Another set of SH-SY5Y cells was placed in a 96-well plate at 2×10^4 cells per well, incubated for 24 h and treated with CoQ10 or CoQ10 Ac (5–10 μM) for 24 h. After incubation, the treatment medium was discarded and cells were treated with 6-OHDA (200 μM) for 2 h at 37 °C in 5 % CO_2. The treatment medium was subsequently replaced with MTT in HBSS (0.5 mg/mL) and then the plate was incubated for 2 h at 37 °C in 5 % CO_2. After washing the cells with HBSS, formazan crystals were solubilized in isopropanol. The amount of formazan was measured at 570 nm, as described above. Previous chemical reactions involving CoQ10, CoQ10 Ac, or 6-OHDA with MTT in the absence of cells have allowed us to exclude the reducing action of the compounds used on MTT. Data were expressed as percentages relative to untreated cells.

2.7. Determination of α-syn aggregation

The aggregation of α-syn was assessed as previously described (Di Martino et al., 2020). Briefly, TagGFP2-α-syn SH-SY5Y cells were placed in a 96-well plate at 2×10^4 cells per well, incubated for 24 h and then treated with CoQ10 or CoQ10 Ac (5–10 μM) in the presence of 6-OHDA (100 μM) for 2 h at 37 °C in 5 % CO_2. At the end of incubation, the aggregation of α-syn was assessed using the inverted fluorescent microscope Eclipse Ti-E (Nikon Instruments Spa, Florence, Italy). The intensity of fluorescence was directly proportional to the aggregation of α-syn. The intensity of fluorescence was measured by NIS Elements Imaging Software (Nikon Instruments Spa). Data were expressed as Relative Fluorescence Units (RFU).

2.8. Confocal laser scanning microscopy (CLSM)

SH-SY5Y cells were placed in 60 mm dishes at 2×10^6 cells per dish, incubated for 24 h and then treated with CoQ10 or CoQ10 Ac (10 μM) for 24 h at 37 °C in 5 % CO_2. After incubation, cells were treated with 6-OHDA for 2 h at 37 °C in 5 % CO_2. Subsequently, cells were pelleted and fixed in 4 % paraformaldehyde in 0.1 M PBS, pH 7.4 for 1 h, before being ready for experimentation. To determine the mitochondrial mass and mitochondria volume, 100 nM MTG for 20 min (Exc-Em = 490/523 nm) or 50 nM NAO for 10 min (Exc-Em = 495/522 nm) were added to the cell culture media, respectively. NAO fluorescence intensity has been quantified using Image J Software on an established cell number (100 cells) for each condition. Slides were finally mounted with an anti-fading medium (Vectashield, Vector Labs). Images were collected with a Leica TCS-SP5 Confocal connected to aDMI 6000 CS Inverted Microscope (Leica Microsystems CMS GmbH) and analyzed using the Leica Application Suite Advanced Fluorescence (LAS AF) software. Samples were examined using oil immersion objective lenses (403 N.A. 1.25; 633 N.A. 1.40). Excitation was at 488 nm (FITC and NAO); emission signals were detected at 519 nm (NAO) or 525 nm (FITC). CLSM images are presented as single-plane images or *Z*-stack projections. Data were expressed as percentages relative to untreated cells.

2.9. Determination of caspase-3, PARP1 and mitochondrial fusion/fission protein levels

Caspase-3 and mitochondrial fusion/fission protein levels were assessed in SH-SY5Y cells using western blotting, as previously described (Pruccoli et al., 2020). Cells were placed in 60 mm dishes at 2×10^6 cells per dish, incubated for 24 h and then treated with CoQ10 or CoQ10 Ac (10 μM) for 24 h at 37 °C in 5 % CO_2. After incubation, cells were treated with 6-OHDA (200 μM) for 2 h and then recovered in fresh cell culture media for 3 h at 37 °C in 5 % CO_2. After recovery, cells were pelleted and a complete lysis buffer containing leupeptin (2 μg/mL), phenylmethanesulfonylfluoride (100 μg/mL) and a cocktail of protease/phosphatase inhibitors (100×) was added. A small amount of the lysate was taken out to determine the protein concentration using the Bradford method. The protein lysates (50 μg per sample) were separated by 12 % SDS polyacrylamide gels (Bio-Rad Laboratories, Hercules, CA, USA) and transferred onto 0.45 μm nitrocellulose membranes. The membranes were then probed with primary caspase-3 (1:1000; catalog no. 9662, Cell Signaling Technology, Danvers, MA, USA) or PARP1 (1:000; catalog no. 9542, Cell Signaling Technology) or OPA1 (1:1000; catalog no. 80471, Cell Signaling Technology) or DRP1 antibody (sc-272,583, Santa Cruz Biotechnology, Dallas, TX, USA) and secondary antibody. Enhanced chemiluminescence reagents (Pierce, Rockford, IL, USA) were used to detect targeted bands. The same membranes were probed with an anti-β-Actin antibody (1:1000; catalog no A1978, Sigma-Aldrich) and a secondary antibody. Densitometry analysis was performed using the Image Lab software (version 5.2, Bio-Rad Laboratories). Data were expressed as a ratio of primary antibody levels to β-Actin protein levels.

2.10. C. elegans strains and maintenance of worms

The strains N2 standard wild-type was obtained from the Caenorhabditis Genetics Center (CGC Elegans) (University of Minnesota, MN, USA). The strains NL5901: pkIs2386 [unc-54p::alphasynuclein::YFP + unc-119(+)] was obtained from the Laboratory of Molecular, Cellular and Genomic Biomedicine, Instituto De Investigación Sanitaria La Fe, Valencia, Spain; Joint Unit for Rare Diseases IIS La Fe-CIPF, 46012 Valencia, Spain. All strains were grown in NGM (0.3 % NaCl, 2 % agar, 0.25 % peptone, 5 mg/mL cholesterol, 1 M KPO4, 1 M MgSO4) agar plates and fed with the bacterium *Escherichia coli* OP50 strain, distributed in a thin layer over the agar. All worm strains were maintained at 20 °C degrees, according to the standard protocol as described elsewhere (Stiernagle, 2006).

2.11. Measurement of α-syn accumulation in NL5901 worms

NL5901 worms of the L4 stage were placed on NGM/OP50 plates with or without CoQ10 or CoQ10 Ac (200 μM) for 48 h. Ten worms were used per plate for each experimental condition. After treatment, worms were placed on 2 % agarose pads, immobilized with a 0.25 M sodium azide drop, and then analyzed by fluorescence microscopy using a Nikon Eclipse Ti—U inverted fluorescence microscope at 20× magnification. The intensity of YFP-fused α-syn in body wall muscle cells was quantified in a defined region of interest (ROI) within each image.

2.12. Thrashing assay in N2 wilde-type worms

To evaluate the effect of CoQ10 and CoQ10 Ac on worm motility, thrashing behavior was assessed in N2 wild-type worms. Worms were either co-treated as young adults on NGM plates containing CoQ10 or CoQ10 Ac (200 μM) together with 50 mM 6-OHDA and 10 mM ascorbic acid for 1 h, or pre-treated from hatching for 72 h on CoQ10 or CoQ10 Ac/OP50/NGM plates and then exposed to 50 mM 6-OHDA and 10 mM ascorbic acid for 1 h. After exposure, all worms were transferred to NGM/OP50 plates for a 3-day recovery. Before scoring, each animal was immersed in 1 mL of M9 buffer for 30 s to acclimatize to the liquid medium. Thrashes were counted for 1 min under a stereomicroscope, and the average was calculated per animal. Twenty worms were used per plate for each experimental condition.

2.13. Statistical analysis

Data were reported as mean ± standard deviation (SD) of at least three independent experiments. Statistical analysis was performed using PRISM 5 software (GraphPad Software, La Jolla, CA, USA). Student's *t*-test and one-way ANOVA with Bonferroni post hoc test were used to determine statistical significance ($p < 0.05$).

3. Results

We initially evaluated the neurotoxicity of various concentrations of CoQ10 and CoQ10 Ac, ranging from 1.25 to 40 μM, in SH-SY5Y cells using the MTT assay to identify the concentrations that would not induce neurotoxicity. The results showed that the treatment of SH-SY5Y cells with either CoQ10 or CoQ10 Ac for 24 h resulted in neurotoxicity only at 40 μM for both compounds (data not shown). Therefore, we selected concentrations lower than 20 μM for the subsequent antioxidant and neuroprotective experiments in SH-SY5Y cells. The antioxidant activity of CoQ10 and CoQ10 Ac, in terms of radical scavenging activity, was initially evaluated without the presence of SH-SY5Y cells. This assessment was conducted using the DPPH and ABTS assays, which analyze reactions with free radicals in two different environments: an organic solution for the DPPH assay and an aqueous buffer solution for the ABTS assay. The experimental conditions of the DPPH assay closely mimic the lipidic environment, such as that found in the cell membrane,

whereas the conditions of the ABTS assay simulate the physiological environment of extracellular spaces and intracellular cytoplasm (Wołosiak et al., 2021).

As shown in Fig. 2A, neither CoQ10 nor CoQ10 Ac exhibited radical scavenging activity against the DPPH radical. However, both compounds showed significant radical scavenging activity against the ABTS radical. Notably, CoQ10 Ac exhibited approximately 2.6-fold higher antioxidant activity than CoQ10 (Fig. 2B). The same ABTS assay was used to evaluate the TAA of membrane and cytoplasmic fractions of SH-SY5Y cells treated with 10 μM CoQ10 and CoQ10 Ac for 2 h. This experimental approach enables the evaluation of the cellular uptake of CoQ10 and CoQ10 Ac, as well as their effectiveness in counteracting free radicals at different subcellular levels. As expected, CoQ10 significantly increased TAA in both fractions compared to untreated cells. Notably, CoQ10 Ac further enhanced TAA, with a significantly greater increase than CoQ10 in both the membrane and cytoplasmic fractions (Fig. 2C and D). These results suggest that CoQ10 Ac exhibits greater radical scavenging activity than CoQ10 in aqueous buffer solution. This aqueous environment readily promotes the hydrolysis of the acetate, resulting in the formation of the active form, CoQ10H2. Even CoQ10 can be partially reduced to CoQ10H2 by certain components present in buffered saline solutions, which promotes redox reactions and justifies the minimal recorded radical scavenging activity (Araoyinbo et al., 2013). Supporting previous studies, CoQ10 did not show radical scavenging activity in an organic solution, similar to CoQ10 Ac (Cervellati and Greco, 2016). These findings imply that both compounds, particularly CoQ10 Ac, have a more helpful aqueous environment for reacting with free radicals at both extracellular and intracellular levels. This is further supported by the significant increase in cytosolic TAA observed in SH-SY5Y cells after treatment with CoQ10 Ac.

To further investigate the antioxidant activity of CoQ10 and CoQ10 Ac, we evaluated their ability to counteract or prevent the intracellular ROS formation elicited by H_2O_2 in SH-SY5Y cells using DCFH-DA assay. As shown in Fig. 3A, treating SH-SY5Y cells with either CoQ10 or CoQ10 Ac (5 and 10 μM) in the presence of H_2O_2 (200 μM) for 30 min significantly decreases the ROS formation at all concentrations used, supporting the TAA recorded for both compounds by ABTS assay. The inhibition of ROS formation correlated with the concentrations of both compounds, and CoQ10 Ac exhibited a slightly higher, although not statistically significant, inhibition than CoQ10 (percentage of inhibition: 71.16 % vs. 60.81 % at 5 μM; 96.58 % vs. 81.77 % at 10 μM). Interestingly, the similar treatment with both CoQ10 and CoQ10 Ac at 5 and 10 μM in the absence of H_2O_2 reduced ROS levels by approximately 30 % (data not shown). This finding suggests that CoQ10 or CoQ10 Ac quickly convert to CoQ10H2, which has antioxidant properties, during their movement into neuronal cells. Conversely, treating SH-SY5Y cells with either CoQ10 or CoQ10 Ac for 24 h before the H_2O_2 exposure of 30 min did not prevent the intracellular ROS formation (Fig. 3B). These results show the ability of both CoQ10 and CoQ10 Ac to counteract only the concomitant ROS formation, suggesting their direct antioxidant activity through the formation of CoQ10H2 at the neuronal level. However, these findings of antioxidant activity do not exclude that CoQ10 and CoQ10 Ac could explain other neuroprotective effects that typically arise from their support of mitochondrial activity.

Subsequently, we assessed the neuroprotective effects of CoQ10 and CoQ10 Ac against the neurotoxicity induced by neurotoxin 6-OHDA in SH-SY5Y cells using the MTT assay. Treatment of SH-SY5Y cells with various concentrations of CoQ10 or CoQ10 Ac (5–10 μM) alongside 6-OHDA (200 μM) significantly reduced neurotoxicity across all concentrations in a dose-dependent manner. Notably, CoQ10 Ac exhibited significantly greater neuroprotective effects than CoQ10 at 10 μM concentration, supporting its higher antioxidant activity (Fig. 4A). Interestingly, prolonged treatment of SH-SY5Y cells for 24 h with CoQ10 Ac, unlike CoQ10, significantly prevented neurotoxicity induced by 6-OHDA at 5 and 10 μM (Fig. 4B).

Based on this evidence, we investigated the activation of PARP1 and caspase-3, which are key mediators of major neuronal death pathways, by western blotting (Hartmann et al., 2000; Liu et al., 2025; Venderova and Park, 2012). As shown in Fig. 5, exposure of cells to 6-OHDA increased the levels of cleaved PARP1 and caspase-3 proteins, both of which play central roles in neuronal death. Pre-treatment of cells with CoQ10 or CoQ10 Ac resulted in a significant reduction in the levels of the cleaved PARP1 and caspase-3 proteins. Notably, CoQ10 Ac demonstrated a greater capability to decrease both cleaved proteins than CoQ10, indicating enhanced neuroprotective effects.

Given the significant neuroprotective effects of CoQ10 Ac against neurotoxicity induced by 6-OHDA, we also examined its impact on mitochondrial dysfunction, a pathological event leading to neuronal death, caused by the same neurotoxin. We initially examined changes in mitochondrial dynamics by assessing the expression of fusion and fission proteins by western blotting. It is believed that a disruption in the balance of the fission and fusion proteins, leading to a high fission protein/fusion protein ratio, can be a critical step in apoptotic neuronal death (Chen et al., 2023). As shown in Fig. 6, exposure of cells to 6-OHDA decreased the expression of the fusion protein OPA1 but increased the expression of the fission protein DRP1. Pre-treatment of cells with CoQ10 or CoQ10 Ac significantly rescued OPA1 protein level, but the same treatment did not have an effect on the expression of DRP1 protein. Both CoQ10 and CoQ10 Ac significantly reduced the increase of the DRP1 (fission protein)/OPA1 (fusion protein) ratio induced by 6-OHDA, suggesting that their antiapoptotic effects contribute to their neuroprotective properties.

Then, mitochondrial dysfunction was assessed using fluorescent probes NAO and MTG, which measure the structural integrity and the mass of the mitochondria, respectively (Doherty and Perl, 2017). The prolonged treatment of SH-SY5Y cells with 10 μM CoQ10 and CoQ10 Ac

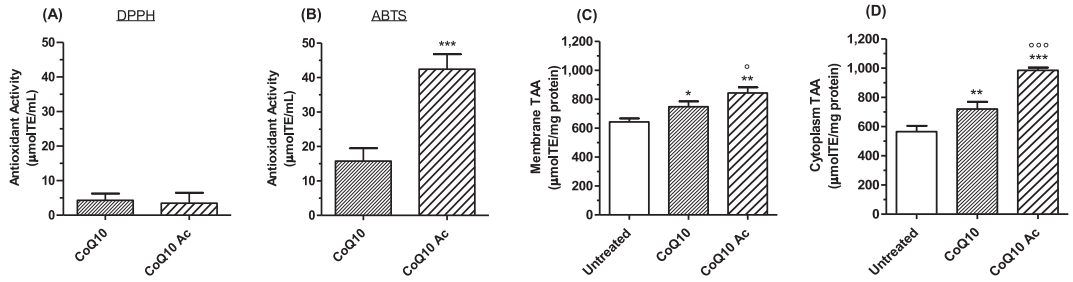

Fig. 2. Antioxidant Activity of CoQ10 and CoQ10 Ac. (A, B) The antioxidant activity of CoQ10 and CoQ10 Ac at a concentration of 10 μM was evaluated using the DPPH and ABTS assay. Data are expressed as micromoles of trolox equivalents per milliliter of compound solution and reported as mean ± SD of three independent experiments (*** $p < 0.001$ vs. CoQ10, Student's *t*-test); (C, D) SH-SY5Y cells were treated for 2 h with CoQ10 or CoQ10 Ac at the concentration of 10 μM. At the end of treatment, the TAA was evaluated in the membrane and cytoplasmic fractions using the ABTS assay. Data are expressed as micromoles of trolox equivalents per milligram of protein and reported as mean ± SD of at least three independent experiments (° $p < 0.05$ and °°° $p < 0.001$ vs. cells treated with CoQ10; * $p < 0.05$, ** $p < 0.01$ and *** $p < 0.001$ vs. untreated cells, one-way ANOVA with Bonferroni post hoc test).

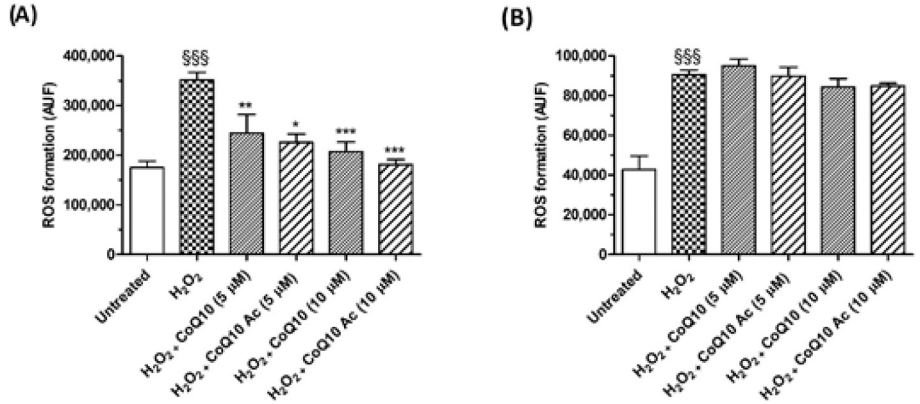

Fig. 3. Effects of CoQ10 and CoQ10 Ac on ROS formation in SH-SY5Y cells. (A) Cells were treated with CoQ10 or CoQ10 Ac (5–10 μM) in the presence of H2O2 (200 μM) for 30 min; (B) cells were treated for 24 h with CoQ10 or CoQ10 Ac (5–10 μM) and then with H2O2 (200 μM) for 30 min. After the different treatments, ROS formation was determined using the fluorescent probe DCFH-DA. Data are expressed as arbitrary units of fluorescence (AUF) and reported as mean ± SD of at least three independent experiments (§§§ $p < 0.001$ vs. untreated cells; * $p < 0.05$, ** $p < 0.01$ and *** $p < 0.001$ vs. cells treated with H2O2, one-way ANOVA with Bonferroni post hoc test).

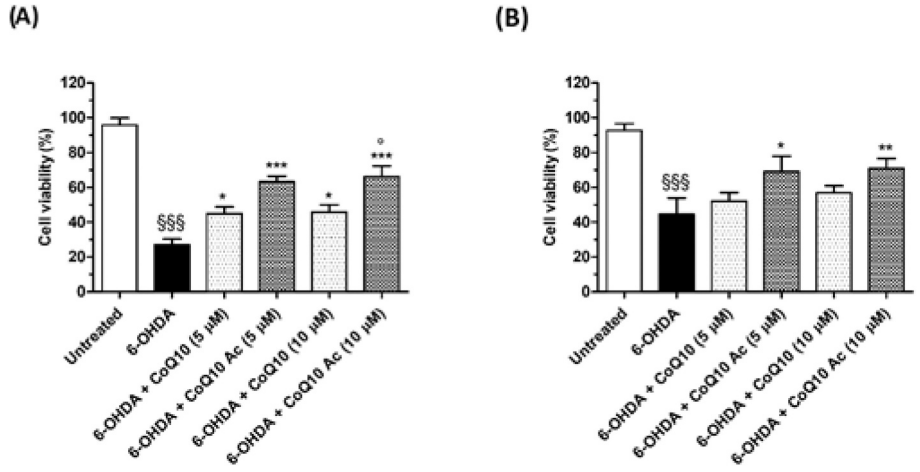

Fig. 4. Neuroprotective effects of CoQ10 and CoQ10 Ac against the neurotoxicity induced by 6-OHDA in SH-SY5Y cells. (A) Cells were treated with CoQ10 or CoQ10 Ac (5–10 μM) in the presence of 6-OHDA (200 μM) for 2 h; (B) cells were treated with CoQ10 or CoQ10 Ac (5–10 μM) for 24 h and then with 6-OHDA (200 μM) for 2 h. After the different treatments, the cell viability was determined using MTT assay. Data are expressed as percentage and reported as mean ± SD of at least three independent experiments (§§§ $p < 0.001$ vs. untreated cells; * $p < 0.05$, ** $p < 0.01$ and *** $p < 0.001$ vs. cells treated with 6-OHDA; ° $p < 0.05$ vs cells treated with 6-OHDA and CoQ10 (10 μM), one-way ANOVA with Bonferroni post hoc test).

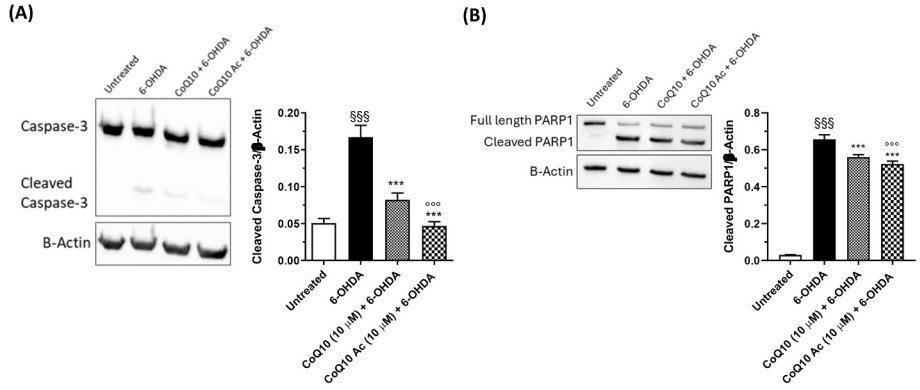

Fig. 5. Effects of CoQ10 and CoQ10 Ac on neuronal death induced by 6-OHDA in SH-SY5Y cells. Cells were treated with CoQ10 or CoQ10 Ac (10 μM) for 24 h and then with 6-OHDA (200 μM) for 2 h. After treatment, cells were recovered in fresh cell culture medium for 3 h. At the end of incubation, caspase-3 (A) and PARP1 (B) protein levels were detected by western blotting. Data were expressed as a ratio of caspase-3 or PARP1 protein levels to β-Actin protein levels and reported as mean ± SD of at least three independent experiments (*** $p < 0.001$ vs. cells treated with 6-OHDA; §§§ $p < 0.001$ vs. untreated cells, °°° $p < 0.001$ vs. cells treated with CoQ10, one-way ANOVA with Bonferroni post hoc test).

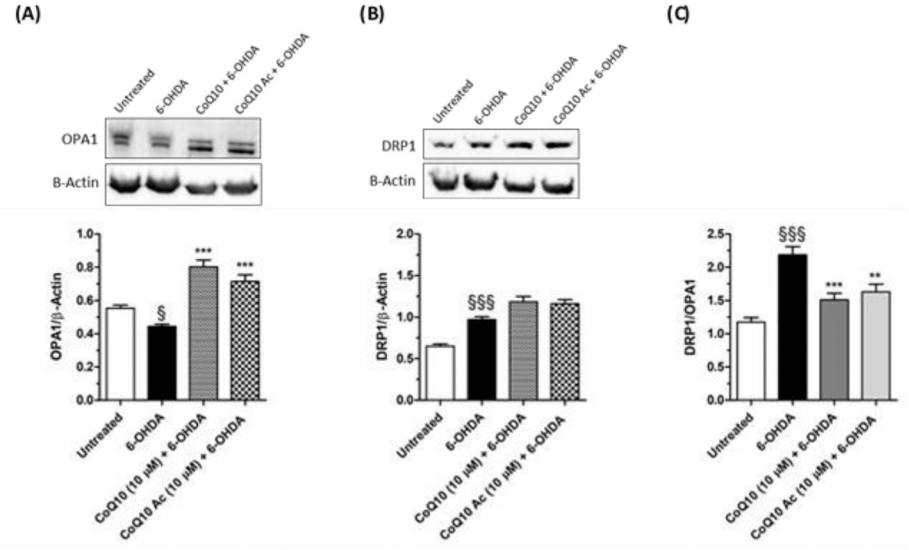

Fig. 6. Effects of CoQ10 and CoQ10 Ac on mitochondrial dynamics imbalance induced by 6-OHDA in SH-SY5Y cells. Cells were treated with CoQ10 or CoQ10 Ac (10 μM) for 24 h and then with 6-OHDA (200 μM) for 2 h. After treatment, cells were recovered in fresh cell culture medium for 3 h. At the end of incubation, mitochondrial fusion (OPA1) (A)/fission (DRP1) (B) protein levels were detected by western blotting; (C) Ratio between DRP1 and OPA1. Data were expressed as a ratio of OPA1 or DRP1 protein levels to β-Actin protein levels and reported as mean ± SD of at least three independent experiments (*** $p < 0.001$ and ** $p < 0.01$ vs. cells treated with 6-OHDA; §§§ $p < 0.001$ and § $p < 0.05$ vs. untreated cells, one-way ANOVA with Bonferroni post hoc test).

significantly prevented the decrease of NAO fluorescence induced by the treatment with 6-OHDA, suggesting their ability to preserve the mitochondrial structural integrity. In particular, we observed high green fluorescence intensity in untreated cells (Fig. 7A), while 6-OHDA-treated cells showed low NAO fluorescence intensity (Fig. 7D). CoQ10 (Fig. 7B) and CoQ10 Ac (Fig. 7C) did not modify the fluorescence of untreated cells. Pretreatment of CoQ10 (Fig. 7E) and CoQ10 Ac (Fig. 7F) maintained the mitochondrial structural integrity against oxidative damage induced by 6-OHDA treatment, as demonstrated by the high fluorescence in both conditions. A quantification of NAO fluorescence intensity was reported in Fig. 7G. High NAO fluorescence indicates the presence of well-preserved mitochondria during low fluorescence degeneration of structural membrane and cardiolipin. In fact, cardiolipin is subjected to peroxide oxidation by cytochrome *c* in the presence of hydroxy dopamine and other chemicals, and oxidized cardiolipin has low affinity for NAO staining. Furthermore, in literature, we can find several pieces of evidence demonstrating that cardiolipin oxidation is related to the apoptotic process (Kagan et al., 2005; Ott et al., 2007); then NAO staining not only provides a direct indication of the structural integrity of the mitochondria but also indirectly suggests the activation of the intrinsic apoptotic pathway.

We also evaluate the effect on mitochondrial mass with MTG fluorescent staining. The high green fluorescence of untreated cells (Fig. 8A) appears low in 6-OHDA-treated cells (Fig. 8D). CoQ10 (Fig. 8B) and CoQ10 Ac (Fig. 8C) did not modify the fluorescence of untreated cells. The pretreatment with CoQ10 (Fig. 8E) or CoQ10 Ac (Fig. 8F) showed a

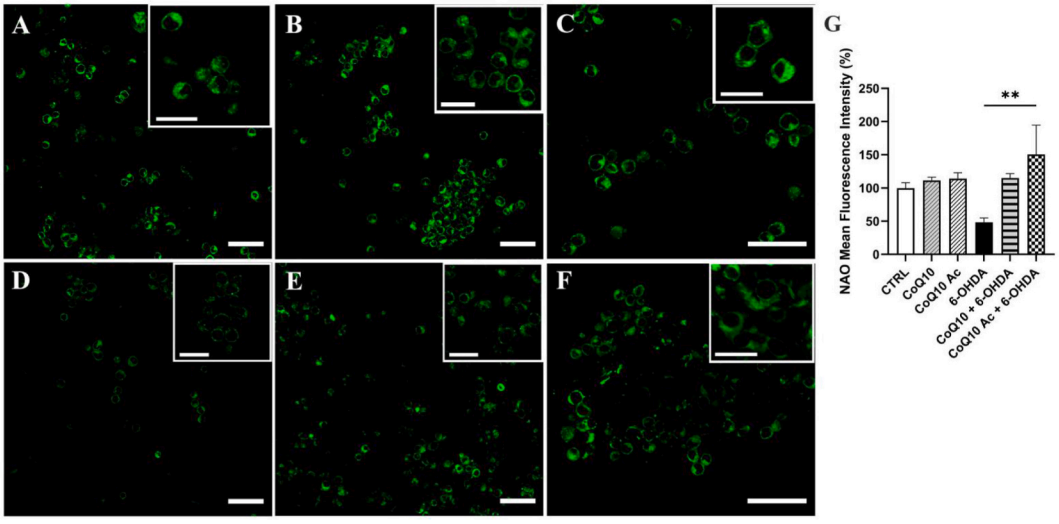

Fig. 7. Effects of CoQ10 and CoQ10 Ac on the loss of mitochondrial structural integrity induced by 6-OHDA in SH-SY5Y cells. (A) Cells were treated with CoQ10 or CoQ10 Ac (10 μM) for 24 h and then with 6-OHDA (100 μM) for 2 h. After treatment, the mitochondrial structural integrity was detected by NAO staining. (G) Data were expressed as percentages relative to untreated cells and reported as mean ± SD of at least three independent experiments (** $p < 0.01$ vs. cells treated with 6-OHDA, one-way ANOVA with Bonferroni post hoc test). Confocal images of NAO staining: (A) untreated cells, (B) cells treated with CoQ10, (C) cells treated with CoQ10 Ac, (D) cells treated with 6-OHDA, (E) cells treated with CoQ10 in the presence of 6-OHDA, (F) cells treated with CoQ10 Ac in the presence of 6-OHDA; (G) quantification of NAO fluorescence intensity. Scale bars: A, E, bar = 100 μm; B - D, bar = 50 μm; F, insert A —F, bar = 25 μm.

partial recovery of the fluorescence affected by 6-OHDA treatment. In particular, the fluorescence recovery was more evident with CoQ10 Ac than CoQ10. A quantification of MTG fluorescence intensity was reported in Fig. 8G. In contrast to the results concerning mitochondrial structural integrity, which showed similar protective effects for both CoQ10 and CoQ10 Ac, the findings related to mitochondrial mass indicate that CoQ10 Ac has a greater capacity to preserve the structure and function of mitochondrial membranes. This suggests that CoQ10 Ac may be more readily available at this level.

We also used similar treatment conditions in green fluorescent α-syn SH-SY5Y cells (TagGFP2-α-syn) with CoQ10 or CoQ10 Ac to evaluate the α-syn aggregation promoted by 6-OHDA. In particular, the fluorescence intensity of α-syn was correlated with its aggregation level in the cytoplasm of TagGFP2-α-syn SH-SY5Y cells and allowed the evaluation of the effects of the different treatments on it. The treatment of TagGFP2-α-syn SH-SY5Y cells with 10 μM of CoQ10 or CoQ10 Ac, applied before or during the treatment with 6-OHDA (100 μM), significantly reduced α-syn aggregation. This suggests that both compounds can counteract or prevent the α-syn aggregation by 6-OHDA-induced oxidative stress (Fig. 9A, B and C).

Lastly, we evaluate some neuroprotective effects of CoQ10 and CoQ10 Ac in the nematode *Caenorhabditis elegans*. This model organism can exhibit several characteristics related to PD, including the loss of dopamine neurons, disruption of dopamine-dependent movement and aggregation of neurotoxic protein such as α-syn (Cooper and Van Raamsdonk, 2018). We used *C. elegans* treated with 6-OHDA, the same neurotoxin employed in SH-SY5Y cells, to induce dopamine neuron dysfunction and impair movement. We measured the thrashing behavior of the worm. As depicted in Fig. 10, treatment with 50 mM of 6-OHDA for 1 h significantly decreased the thrashing activity of the worm. The concomitant treatment with CoQ10 Ac (200 μM) partially restored thrashing, suggesting neuroprotective effects on dopaminergic functions, whereas CoQ10 (200 μM) did not have this effect. Furthermore, treating the worms with both compounds for 3 days before the treatment with 6-OHDA led to a significant reduction in impaired thrashing, approaching almost total recovery of the movement. These findings suggest that chronic exposure enhances the neuroprotective effects of both compounds. We also evaluated the α-syn aggregation in *C. elegans* expressing YFP-fused human α-syn, referred to as NL5901 worms. Treatment with CoQ10 Ac (200 μM) for 2 days significantly reduced α-syn aggregation in NL5901 worms, confirming its ability to inhibit the aggregation as observed in SH-SY5Y cells (Fig. 11). In contrast, CoQ10 did not show any anti-aggregant effects in NL5901 worms, suggesting that CoQ10 Ac has greater bioavailability than CoQ10, enabling it to reach the human α-syn::YFP in muscle cells of the worm more effectively.

4. Discussion

Our study has evaluated, for the first time, the effectiveness of CoQ10 and CoQ10 Ac in counteracting ABTS radicals, specifically focusing on TAA at the membrane and cytoplasmic levels of the SH-SY5Y cells treated with the studied compounds. This experimental approach demonstrated that CoQ10 Ac exhibited a greater capacity to increase the TAA within the membrane and, particularly, the cytoplasm than CoQ10. This suggests a distinct formation of reduced active forms, CoQ10H2, from CoQ10 and CoQ10 Ac at the different subcellular levels. Notably, CoQ10 and CoQ10 Ac have similar liposolubility values, with logP values of 17.76 and 17.898, respectively, as determined by ADMETlab 3.0 for in silico prediction (Fu et al., 2024). Furthermore, the in silico ADME (Absorption, Distribution, Metabolism, and Excretion) parameters showed favourable properties for oral absorption and the ability to permeate across the blood-brain barrier (Supplementary Table 1). This suggests that they have a comparable ability to move across biological membranes, including the ability to move within cells. Consequently, the differences in TAA may result from variations in the formation of CoQ10H2, which occurs through the enzymatic processes of reduction and ester hydrolysis acting on CoQ10 and CoQ10 Ac at both the membrane and cytoplasmic levels. Once inside the cells, several enzyme systems that can reduce CoQ10 to CoQ10H2 have been identified (Mantle et al., 2024; Mantle and Dybring, 2020). Notably, DT-diaphorase (also referred to as NOQ1 or NAD(*P*)H: quinone acceptor oxidoreductase) functions as a component of the plasma membrane redox system. Additionally, mitochondrial redox cycle activity and extramitochondrial oxidoreductase enzymes (for example, lipoamide dehydrogenase, glutathione reductase, and seleno-enzyme thioredoxin reductase) act at the cytoplasmic level. Unlike CoQ10, CoQ10 Ac can initially generate CoQ10H2 without relying on reducing enzymes, utilizing esterases present in the membrane, cytoplasm, or cellular organelles, such as mitochondria (Oda et al., 2015; Perrier et al., 2002; Su

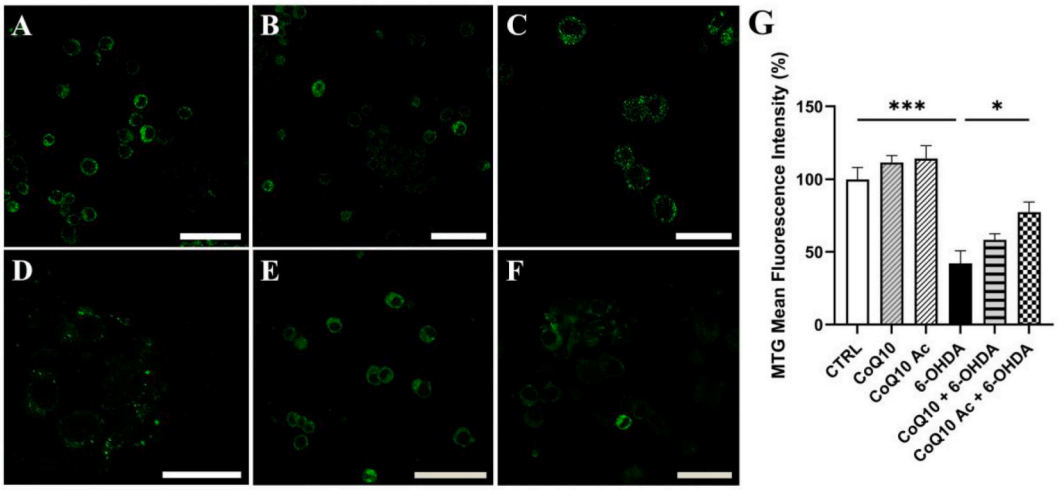

Fig. 8. Effects of CoQ10 and CoQ10 Ac on the loss of mitochondrial mass induced by 6-OHDA in SH-SY5Y cells. (A) Cells were treated with CoQ10 or CoQ10 Ac (10 μM) for 24 h and then with 6-OHDA (100 μM) for 2 h. After treatment, the mitochondrial mass was detected by MTG staining. (G) Data were expressed as percentages relative to untreated cells and reported as mean ± SD of at least three independent experiments (*** $p < 0.001$ vs. untreated cells, * $p < 0.05$ vs. cells treated with 6-OHDA, one-way ANOVA with Bonferroni post hoc test). Confocal images of MTG staining: (A) untreated cells, (B) cells treated with CoQ10, (C) cells treated with CoQ10 Ac, (D) cells treated with 6-OHDA, (E) cells treated with CoQ10 in the presence of 6-OHDA, (F) cells treated with CoQ10 Ac in the presence of 6-OHDA; (G) quantification of MTG fluorescence intensity. Scale bars: A, C, bar = 50 μm; B, D - F, bar = 25 μm.

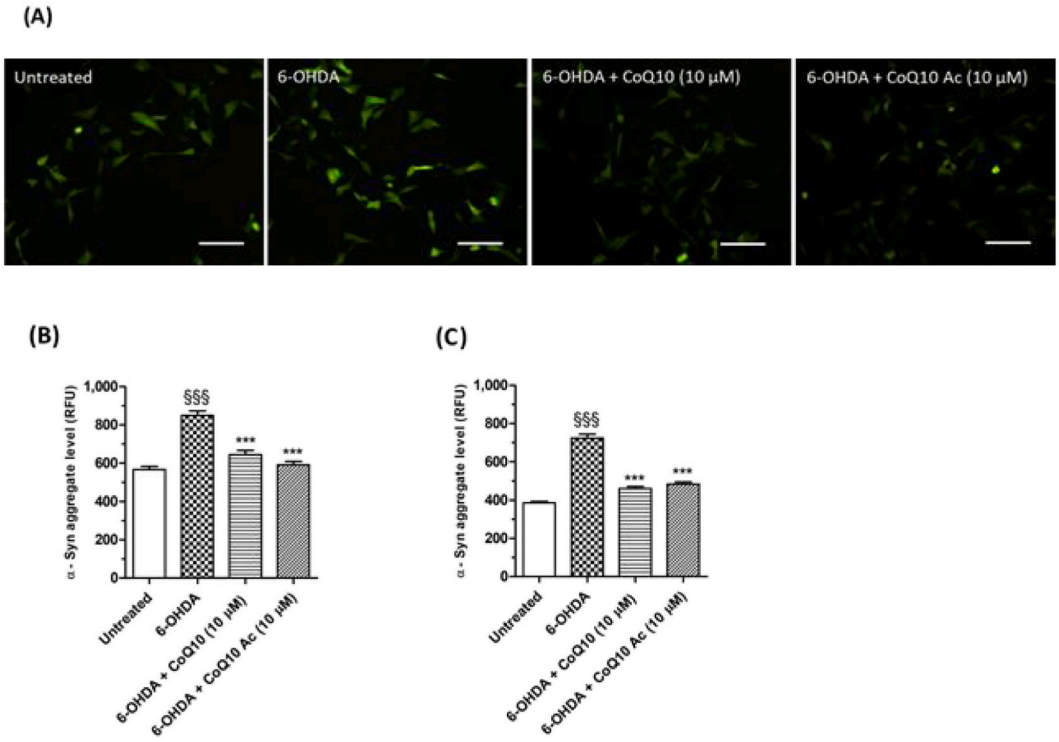

Fig. 9. Effects of CoQ10 and CoQ10 Ac on α-syn aggregates induced by 6-OHDA in TagGFP2-α-syn SH-SY5Y cells. (A) Representative images of α-syn aggregates; (B) cells were treated with CoQ10 or CoQ10 Ac (10 μM) in the presence of 6-OHDA (100 μM) for 2 h; (C) cells were treated with CoQ10 or CoQ10 Ac (10 μM) for 24 h and then with 6-OHDA (100 μM) for 2 h. After the different treatments, the α-syn aggregate level was detected by fluorescence microscope. Data are expressed as relative fluorescence units (RFU) and reported as mean ± SD of at least three independent experiments (§§§ $p < 0.001$ vs. untreated cells; *** $p < 0.001$ vs. cells treated with 6-OHDA, one-way ANOVA with Bonferroni post hoc test). Scale bars: 50 μm.

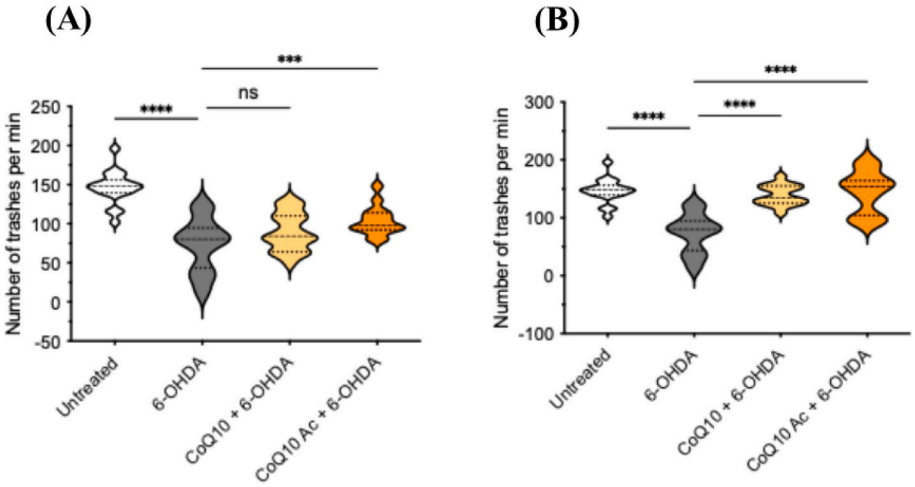

Fig. 10. Effects of CoQ10 and CoQ10 Ac on 6-OHDA-induced thrashing impairment in *C. elegans*. (A) N2 wild-type worms were co-treated with CoQ10 or CoQ10 Ac (200 μM) and 6-OHDA (50 mM) for 1 h at 20 °C at the young adult stage. After 3 days of recovery, worm motility was assessed using the thrashing assay. (B) N2 wild-type worms were pre-treated for 72 h with CoQ10 or CoQ10 Ac (200 μM) and subsequently exposed to 6-OHDA (50 mM) for 1 h at the young adult stage. After 3 days of recovery, worm motility was assessed using the thrashing assay. Data are expressed as the mean of 30 worms and reported as mean ± SD of at least three independent experiments (*** $p < 0.001$, **** $p < 0.0001$ and ns, not significant, one-way ANOVA with Bonferroni post hoc test).

et al., 2024). Based on these highlights, we can therefore speculate that CoQ10 Ac may act as a functional substrate of esterases at neuronal levels, resulting in higher levels of CoQ10H2 in both the membrane and cytoplasm than the reducing enzymatic pathway for CoQ10. Since the continuous interconversion between the CoQ10 and CoQ10H2 forms is required for the normal function of CoQ10, we then assessed the impact of CoQ10H2 formation before or during oxidative stress, in terms of intracellular ROS formation elicited by H_2O_2 in the SH-SY5Y cells. The combined treatment of the SH-SY5Y cells with CoQ10 or CoQ10 Ac and H_2O_2, which resembles the formation of CoQ10H2 during the ROS formation, recorded a strong antioxidant activity with both coenzymes. While CoQ10 Ac demonstrated higher TAA in the cytoplasm compared to CoQ10, its ability to counteract oxidative stress at the intracellular level was similar to that of CoQ10. This suggests that the increased

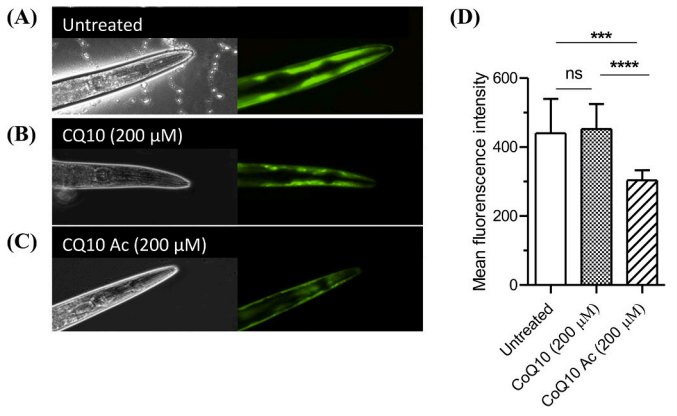

Fig. 11. Effects of CoQ10 and CoQ10 Ac on α-syn aggregation in *C. elegans*. (A–C) Fluorescence images of day-1 adult NL5901 worms expressing YFP-fused human α-syn in body wall muscle cells after 48 h of treatment with CoQ10 or CoQ10 Ac (200 μM). (D) Fluorescence intensity of YFP was quantified in a defined region of interest (ROI) within each image using ImageJ software. Data are expressed as the mean of 30 worms and reported as mean ± SD of at least three independent experiments (*** $p < 0.001$, ****$p < 0.0001$ and ns, not significant, one-way ANOVA with Bonferroni post hoc test).

CoQ10H2 levels generated by CoQ10 Ac may be partially offset by the redox processes triggered by H_2O_2. It is plausible that the cytoplasmatic oxidation of CoQ10H2 can limit its antioxidant action and hinder the enzymatic reduction processes in the redox cycle between CoQ10 and CoQ10H2 as oxidative stress progresses. These observations are further supported by the lack of antioxidant activity when the SH-SY5Y cells were continuously treated for 24 h with either CoQ10 or CoQ10 Ac before the ROS formation induced by H_2O_2. This inability of both CoQ10 and CoQ10 Ac to prevent oxidative stress may be ascribed to the depletion of the antioxidant CoQ10H2 form in neuronal cells and their lack of efficacy in enhancing endogenous antioxidant defences. Notably, our results also indicate that CoQ10 Ac has greater neuroprotective effects than CoQ10 against neurotoxicity induced by the neurotoxin 6-OHDA. This conclusion is based on both concomitant treatment and pre-treatment outcomes observed through the MTT assay, suggesting that these effects occur at the mitochondrial level. CoQ10 Ac also showed a higher ability to inhibit the activation of PARP1 and caspase-3 than CoQ10. This finding is significant, as post-mortem studies of the human brain have shown that PARP1 and caspase-3 are key vulnerability factors in the neuronal death of dopaminergic neurons in PD. These studies have further recorded a PARP1 colocalizes with α-syn in the cytoplasm and in Lewy bodies of PD tissue sections, supporting the pathological role of PARP1 to promote the formation of pathologic α-syn resulting in neuronal death (Kam et al., 2018). We therefore evaluated the toxic events starting from mitochondrial dysfunction, including the impairment of mitochondrial fusion and fission as well as the loss of mitochondrial structural integrity and mass, to α-syn aggregation, which ultimately leads to the complete degeneration of dopaminergic neurons in PD. In this regard, CoQ10 and CoQ10 Ac lower the increase of the DRP1 (fission protein)/OPA1 (fusion protein) ratio induced by 6-OHDA in SH-SY5Y cells through their strong ability to increase OPA1 fusion protein, leading to antiapoptotic death. OPA1 is crucial for mitochondrial fusion, integrity, and cristae structure, and it prevents cytochrome *c* release, thereby inhibiting the apoptotic cascade (Lin et al., 2020). CoQ10 Ac demonstrated a higher ability to maintain mitochondrial structural integrity and mitochondrial mass compared to CoQ10, highlighting its potential higher localization of CoQ10H2 at the mitochondrial level. A pharmacokinetic study evaluated the distribution of total CoQ10 (including CoQ10 and CoQ10H2) in subcellular fraction of guinea pig after oral administration of CoQ10 or CoQ10 Ac. The finding showed that total CoQ10 is mainly distributed in the nuclei, heavy mitochondria, and lysosomes (Passi et al., 2003). Notably, the total CoQ10 levels in the nuclei and in the mitochondria were higher with CoQ10 Ac compared to CoQ10 oral administration, showing percentage increases of 32 % vs 7 % and 35 % vs 29 %, respectively. Since cardiolipin is a specific phospholipid found in the inner mitochondrial membrane, it plays a crucial role in regulating electron transfer between complex I and CoQ10. The improved protective effects of CoQ10 Ac on mitochondrial structural integrity, compared to CoQ10, may be attributed to its conversion into CoQ10H2 and subsequent reversion to CoQ10. This transformation helps prevent the oxidation of cardiolipin and supports the role of CoQ10 as an electron carrier between complex I and complex III (Paradies et al., 2014). It is noteworthy that CoQ10 Ac has a unique ability to increase both CoQ10 and CoQ10H2 at nuclear level. This suggests a transcriptional regulation of several genes involved in mitochondrial biogenesis, which further supports our findings of increased mitochondrial mass after treatment with CoQ10 (Clemente-Suárez et al., 2023). In this context, a recent study demonstrates that CoQ10 Ac can upregulate the expression of genes associated with mitochondrial biogenesis, including PGC-1α and TFAM (Micucci et al., 2025). Finally, CoQ10 and CQ10 Ac showed a similar ability to counteract α-syn aggregation in SH-SY5Y cells when administered both during and before treatment with 6-OHDA. It is important to note that the oxidative stress triggered by 6-OHDA promotes α-syn aggregation, disrupts mitochondrial integrity through interactions with cardiolipin, impairs the translocase of the mitochondrial outer membrane (TOM20) complex, inhibits complex I activity, and drives ROS production. These events further exacerbate protein aggregation and amplify neuronal damage (Di Maio et al., 2016; Rocha et al., 2018). The ability of CoQ10 and CoQ10 Ac to reduce α-syn aggregation during 6-OHDA treatment can be primarily attributed to their ability to mitigate the oxidative stress, as evidenced by their antioxidant activity recorded against H_2O_2 during concurrent treatment. Recent studies have shown that the intracellular H_2O_2 produced by 6-OHDA in rats is a significant trigger for the degeneration of nigral dopaminergic neurons, and H_2O_2 plays a dominant role in the aggregation of α-syn in an *in vitro* model (Nishio et al., 2022; Xu et al., 2015). Although treating SH-SY5Y cells with both compounds before exposure to oxidative stress via H_2O_2 did not show antioxidant activity, this pre-treatment condition reduced α-syn aggregation. This suggests there are anti-aggregant mechanisms that operate independently of their antioxidant activity. A recent study has demonstrated that hydrophobic antioxidants, such as vitamin A, ß-carotene and CoQ10, may have anti-fibrillogenic effects due to hydrophobic–hydrophobic interactions (Ono and Yamada, 2007). Specifically, CoQ10 has been shown to dose-dependently inhibit the formation of α-syn fibrils from fresh α-syn and destabilized preformed α-syn fibrils in vitro. However, among CoQ10 and CoQ10 Ac, only CoQ10 Ac has been shown to inhibit the aggregation of α-syn in a transgenic *C. elegans* model expressing YFP-fused human α-syn. This model mimics an *in vivo* environment and suggests that CoQ10 Ac has a greater ability to distribute at the muscle level, where the α-syn protein is mainly localized in these transgenic worms. Taken together, the results show that CoQ10 Ac has an antioxidant activity at the membrane and neuronal cytoplasm as well as neuroprotective activity against 6-OHDA-induced neuronal death better than CoQ10. Remarkably, the enhanced neuroprotective effects of CoQ10 Ac were also observed in *C. elegans* under stress mediated by 6-OHDA, where it completely restored the impaired behaviours associated with the dysfunction and death of dopaminergic neurons. Furthermore, CoQ10 Ac demonstrates a greater ability to preserve the structure and function of mitochondria, suggesting a synergistic neuroprotective action that combines its antioxidant properties at the cytoplasmic level with support for mitochondrial function under the neurotoxic effects of 6-OHDA. These findings are aligned with the biochemical mechanism behind 6-OHDA toxicity, which highlights that it forms free radicals independently of its significant inhibition of mitochondrial respiratory chain complexes I and IV, although these mechanisms may act synergistically in vivo (Glinka et al., 1997). Recent studies have shown that CoQ10 Ac can overcome the chemical

instability of CoQ10H2 and improve the bioavailability of CoQ10 (Turunen et al., 1999; Umesh et al., 2023). Our results also emphasize that CoQ10 Ac is intriguing due to its potential as a prodrug, activated by esterases. It has been demonstrated that ester derivatives of CoQ10H2 can enhance the intestinal absorption of CoQ10H2 in rats, as well as improve the delivery of CoQ10H2 to keratinocytes after effective uptake in their ester forms and subsequent hydrolysis of the ester bonds within the cells (Setoguchi et al., 2020a, 2020b). Using ester derivatives of CoQ10H2 could be a promising strategy to overcome limitations associated with the neuroprotective effects of CoQ10 in PD, such as low bioavailability and varying individual abilities to convert CoQ10 into the active CoQ10H2 at the brain level. Abnormalities in the DT-diaphorase have been linked to the pathophysiological mechanisms of multiple neurological disorders, including Parkinson's disease (Yuhan et al., 2024). However, the distribution of CoQ10 at the brain level remains a challenge, which may be addressed through the use of new micro- and nano-delivery systems (Choi and McClements, 2020; Hong et al., 2025). All these findings, including those recorded in *C. elegans*, need to be addressed in in vivo rodent models of PD.

5. Conclusions

This study shows that CoQ10 Ac, an esterified form of CoQ10, has superior antioxidant and neuroprotective properties compared to CoQ10 in both the dopaminergic SH-SY5Y cell line and *Caenorhabditis elegans* models of PD. CoQ10 Ac increased cellular TAA and provided stronger protection against mitochondrial dysfunction and neuronal death from 6-OHDA in SH-SY5Y cells. CoQ10 Ac also demonstrated a greater capability to decrease both cleaved caspase-3 and PARP1 proteins than CoQ10, indicating enhanced neuroprotective effects. It was more effective in maintaining mitochondrial integrity and mass, supporting its potential as both an antioxidant and mitochondrial modulator. Notably, CoQ10 Ac inhibited the aggregation of α-syn in a transgenic *C. elegans* model, suggesting a greater ability to distribute at the muscle level compared to CoQ10. The enhanced neuroprotective effects of CoQ10 Ac were also observed in *C. elegans* under stress mediated by 6-OHDA, where it completely restored the impaired behaviours associated with the dysfunction and death of dopaminergic neurons. The conversion of CoQ10 Ac to the active antioxidant form, CoQ10H2, through esterase activity at neuronal levels, may overcome limitations of current CoQ10 supplementation, particularly in individuals with low reducing enzyme activity and neurodegenerative diseases, such as PD. Given its promising neuroprotective profile, CoQ10 Ac is a compelling prodrug candidate for further preclinical investigation as a potential therapeutic agent for PD.

CRediT authorship contribution statement

Matteo Micucci: Writing – original draft, Supervision, Project administration, Funding acquisition, Conceptualization. **Michela Battistelli:** Supervision, Software, Project administration, Funding acquisition, Conceptualization. **Sabrina Burattini:** Software, Methodology, Formal analysis, Data curation. **Riham Osman:** Software, Methodology. **Francesco Onesimo:** Methodology. **Michele Mari:** Visualization, Validation, Conceptualization. **Michele Retini:** Validation. **Ilaria Versari:** Investigation. **Barbara Pagliarani:** Investigation. **Andrea Tarozzi:** Writing – original draft, Visualization, Validation, Supervision, Resources, Investigation, Data curation, Conceptualization. **Giovanni Zappia:** Project administration. **Federico Gianfanti:** Writing – original draft, Visualization. **Letizia Pruccoli:** Writing – original draft, Visualization, Validation, Software, Methodology, Investigation, Formal analysis, Data curation.

Funding sources

This research did not receive any specific grant from funding agencies in the public, commercial, or not-for-profit sectors.

Declaration of competing interest

The authors have no relevant financial or non-financial interests to disclose.

Acknowledgements

The authors would like to thank Samuela Capellacci, University of Urbino Carlo Bo, and Rafael P Vázquez-Manrique, Laboratory of Molecular, Cellular and Genomic Biomedicine, Instituto de Investigación Sanitaria La Fe, for his support in managing *C. elegans*.

Appendix A. Supplementary data

Supplementary data to this article can be found online at https://doi.org/10.1016/j.yexmp.2026.105023.

Data availability

Data will be made available on request.

References

Andrew, R., Watson, D.G., Best, S.A., Midgley, J.M., Wenlong, H., Petty, R.K.H., 1993. The determination of hydroxydopamines and other trace amines in the urine of Parkinsonian patients and normal controls. Neurochem. Res. 18, 1175–1177. https://doi.org/10.1007/BF00978370.

Araoyinbo, A.O., Derman, M.N.B., Rahmat, A., Rafezi Ahmad, K., 2013. Electrochemical measurement of PBS using cyclic voltammetry and AAO fabricated at ambient temperature and low potential. Adv. Mater. Res. 795, 654–657. https://doi.org/10.4028/www.scientific.net/AMR.795.654.

Blum, D., Torch, S., Lambeng, N., Nissou, M.-F., Benabid, A.-L., Sadoul, R., Verna, J.-M., 2001. Molecular pathways involved in the neurotoxicity of 6-OHDA, dopamine and MPTP: contribution to the apoptotic theory in Parkinson's disease. Prog. Neurobiol. 65, 135–172. https://doi.org/10.1016/S0301-0082(01)00003-X.

Borsche, M., Pereira, S.L., Klein, C., Grünewald, A., 2021. Mitochondria and Parkinson's disease: clinical, molecular, and translational aspects. J. Parkinsons Dis. https://doi.org/10.3233/JPD-201981.

Brizi, C., Santulli, C., Micucci, M., Budriesi, R., Chiarini, A., Aldinucci, C., Frosini, M., 2016. Neuroprotective effects of Castanea sativa mill. Bark extract in human neuroblastoma cells subjected to oxidative stress. J. Cell. Biochem. 117, 510–520. https://doi.org/10.1002/jcb.25302.

Cervellati, R., Greco, E., 2016. In vitro antioxidant activity of ubiquinone and ubiquinol, compared to vitamin E. Helv. Chim. Acta 99, 41–45. https://doi.org/10.1002/hlca.201500124.

Chen, W., Zhao, H., Li, Y., 2023. Mitochondrial dynamics in health and disease: mechanisms and potential targets. Signal Transduct. Target. Ther. https://doi.org/10.1038/s41392-023-01547-9.

Chiaino, E., Micucci, M., Cosconati, S., Novellino, E., Budriesi, R., Chiarini, A., Frosini, M., 2020. Olive leaves and hibiscus flowers extracts-based preparation protect brain from oxidative stress-induced injury. Antioxidants 9, 1–15. https://doi.org/10.3390/antiox9090806.

Chiaino, E., Stella, R., Peggion, C., Micucci, M., Budriesi, R., Mattioli, L.B., Marzetti, C., Pessina, F., Valoti, M., Frosini, M., 2022. Acacia catechu willd. Extract protects neuronal cells from oxidative stress-induced damage. Antioxidants 11. https://doi.org/10.3390/antiox11010081.

Choi, S.J., McClements, D.J., 2020. Nanoemulsions as delivery systems for lipophilic nutraceuticals: strategies for improving their formulation, stability, functionality and bioavailability. Food Sci. Biotechnol. https://doi.org/10.1007/s10068-019-00731-4.

Clemente-Suárez, V.J., Redondo-Flórez, L., Beltrán-Velasco, A.I., Ramos-Campo, D.J., Belinchón-deMiguel, P., Martinez-Guardado, I., Dalamitros, A.A., Yáñez-Sepúlveda, R., Martín-Rodríguez, A., Tornero-Aguilera, J.F., 2023. Mitochondria and brain disease: a comprehensive review of pathological mechanisms and therapeutic opportunities. Biomedicines. https://doi.org/10.3390/biomedicines11092488.

Cooper, J.F., Van Raamsdonk, J.M., 2018. Modeling Parkinson's disease in *C. elegans*. J. Parkinsons Dis. 8, 17–32. https://doi.org/10.3233/JPD-171258.

Curtius, H.Ch., Wolfensberger, M., Steinmann, B., Redweik, U., Siegfried, J., 1974. Mass fragmentography of dopamine and 6-hydroxydopamine. J. Chromatogr. A 99, 529–540. https://doi.org/10.1016/S0021-9673(00)90882-3.

Di Maio, R., Barrett, P.J., Hoffman, E.K., Barrett, C.W., Zharikov, A., Borah, A., Hu, X., McCoy, J., Chu, C.T., Burton, E.A., Hastings, T.G., Greenamyre, J.T., 2016. α-synuclein binds to TOM20 and inhibits mitochondrial protein import in Parkinson's disease. Sci. Transl. Med. https://doi.org/10.1126/scitranslmed.aaf3634.

Di Martino, R.M.C., Pruccoli, L., Bisi, A., Gobbi, S., Rampa, A., Martinez, A., Pérez, C., Martinez-Gonzalez, L., Paglione, M., Di Schiavi, E., Seghetti, F., Tarozzi, A.,

Belluti, F., 2020. Novel curcumin-diethyl fumarate hybrid as a dualistic GSK-3β inhibitor/Nrf2 inducer for the treatment of Parkinson's disease. ACS Chem. Neurosci. 11, 2728–2740. https://doi.org/10.1021/acschemneuro.0c00363.
Doherty, E., Perl, A., 2017. Measurement of mitochondrial mass by flow cytometry during oxidative stress. React. Oxy. Spec. https://doi.org/10.20455/ros.2017.839.
Fu, L., Shi, S., Yi, J., Wang, N., He, Y., Wu, Z., Peng, J., Deng, Y., Wang, W., Wu, C., Lyu, A., Zeng, X., Zhao, W., Hou, T., Cao, D., 2024. ADMETlab 3.0: an updated comprehensive online ADMET prediction platform enhanced with broader coverage, improved performance, API functionality and decision support. Nucleic Acids Res. 52, W422–W431. https://doi.org/10.1093/nar/gkae236.
Galindo, M.F., Saez-Atienzar, S., Solesio, M.E., Jordán, J., 2014. 6-Hydroxydopamine as preclinical model of Parkinson's disease. In: Handbook of Neurotoxicity. Springer New York, New York, NY, pp. 639–651. https://doi.org/10.1007/978-1-4614-5836-4_5.
Ghosh, A., Chandran, K., Kalivendi, S.V., Joseph, J., Antholine, W.E., Hillard, C.J., Kanthasamy, Arthi, Kanthasamy, Anumantha, Kalyanaraman, B., 2010. Neuroprotection by a mitochondria-targeted drug in a Parkinson's disease model. Free Radic. Biol. Med. 49, 1674–1684. https://doi.org/10.1016/j.freeradbiomed.2010.08.028.
Glinka, Y., Gassen, M., Youdim, M.B., 1997. Mechanism of 6-hydroxydopamine neurotoxicity. J. Neural Transm. Suppl. 50, 55–66. https://doi.org/10.1007/978-3-7091-6842-4_7.
Hartmann, A., Hunot, S., Michel, P.P., Muriel, M.P., Vyas, S., Faucheux, B.A., Mouatt-Prigent, A., Turmel, H., Srinivasan, A., Ruberg, M., Evan, G.I., Agid, Y., Hirsch, E.C., 2000. Caspase-3: a vulnerability factor and final effector in apoptotic death of dopaminergic neurons in Parkinson's disease. Proc. Natl. Acad. Sci. USA 97, 2875–2880. https://doi.org/10.1073/pnas.040556597.
Hong, R., Han, Y., Chen, S., 2025. Advances in micro- and nano- delivery systems for increasing the stability, bioavailability and bioactivity of coenzyme Q10. Crit. Rev. Food Sci. Nutr. 1–18. https://doi.org/10.1080/10408398.2025.2450543.
Kagan, V.E., Tyurin, V.A., Jiang, J., Tyurina, Y.Y., Ritov, V.B., Amoscato, A.A., Osipov, A. N., Belikova, N.A., Kapralov, A.A., Kini, V., Vlasova, I.I., Zhao, Q., Zou, M., Di, P., Svistunenko, D.A., Kurnikov, I.V., Borisenko, G.G., 2005. Cytochrome C acts as a cardiolipin oxygenase required for release of proapoptotic factors. Nat. Chem. Biol. 1, 223–232. https://doi.org/10.1038/nchembio727.
Kam, T.-I., Mao, X., Park, H., Chou, S.-C., Karuppagounder, S.S., Umanah, G.E., Yun, S.P., Brahmachari, S., Panicker, N., Chen, R., Andrabi, S.A., Qi, C., Poirier, G.G., Pletnikova, O., Troncoso, J.C., Bekris, L.M., Leverenz, J.B., Pantelyat, A., Ko, H.S., Rosenthal, L.S., Dawson, T.M., Dawson, V.L., 2018. Poly(ADP-ribose) drives pathologic α-synuclein neurodegeneration in Parkinson's disease. Science 1979, 362. https://doi.org/10.1126/science.aat8407.
Lin, C.Y., Chen, W.J., Fu, R.H., Tsai, C.W., 2020. Upregulation of OPA1 by carnosic acid is mediated through induction of IKKγ ubiquitination by parkin and protects against neurotoxicity. Food Chem. Toxicol. 136. https://doi.org/10.1016/j.fct.2019.110942.
Liu, C., Lai, F., Zhang, T., Mao, K., Wan, H., He, Y., 2025. Roles and therapeutic potential of PARP-1 in neurodegenerative diseases. Biochem. Pharmacol. 242, 117373. https://doi.org/10.1016/j.bcp.2025.117373.
Mantle, D., Dybring, A., 2020. Bioavailability of coenzyme q10: an overview of the absorption process and subsequent metabolism. Antioxidants. https://doi.org/10.3390/antiox9050386.
Mantle, D., Dewsbury, M., Hargreaves, I.P., 2024. The ubiquinone-ubiquinol redox cycle and its clinical consequences: an overview. Int. J. Mol. Sci. https://doi.org/10.3390/ijms25126765.
Micucci, M., Gianfanti, F., Donati Zeppa, S., Annibalini, G., Canonico, B., Fanelli, F., Saltarelli, R., Osman, R., Montanari, M., Lopez, D., Nasoni, G., Panza, G., Bargagni, E., Luchetti, F., Retini, M., Mari, M., Zappia, G., Stocchi, V., Bartolacci, A., Burattini, S., Battistelli, M., 2025. Q-Der: a next-generation CoQ10 analogue supercharging neuroprotection by combating oxidative stress and enhancing mitochondrial function. Front. Mol. Biosci. 12. https://doi.org/10.3389/fmolb.2025.1525103.
Millichap, L., Turton, N., Damiani, E., Marcheggiani, F., Orlando, P., Silvestri, S., Tiano, L., Hargreaves, I.P., 2024. The effect of neuronal CoQ10 deficiency and mitochondrial dysfunction on a rotenone-induced neuronal cell model of Parkinson's disease. Int. J. Mol. Sci. 25, 6622. https://doi.org/10.3390/ijms25126622.
Mischley, L.K., Allen, J., Bradley, R., 2012. Coenzyme Q10 deficiency in patients with Parkinson's disease. J. Neurol. Sci. 318, 72–75. https://doi.org/10.1016/j.jns.2012.03.023.
Moradi Vastegani, S., Nasrolahi, A., Ghaderi, S., Belali, R., Rashno, M., Farzaneh, M., Khoshnam, S.E., 2023. Mitochondrial dysfunction and Parkinson's disease: pathogenesis and therapeutic strategies. Neurochem. Res. 48, 2285–2308. https://doi.org/10.1007/s11064-023-03904-0.
Müller, T., Büttner, T., Gholipour, A.F., Kuhn, W., 2003. Coenzyme Q10 supplementation provides mild symptomatic benefit in patients with Parkinson's disease. Neurosci. Lett. 341, 201–204. https://doi.org/10.1016/S0304-3940(03)00185-X.
Negida, A., Menshawy, A., El Ashal, G., Elfouly, Y., Hani, Y., Hegazy, Y., El Ghonimy, S., Fouda, S., Rashad, Y., 2016. Coenzyme Q10 for patients with Parkinson's disease: a systematic review and meta-analysis. CNS Neurol. Disord. Drug Targets 15, 45–53. https://doi.org/10.2174/1871527314666150821103306.
Nishio, R., Morioka, H., Takeuchi, A., Saeki, N., Furuhata, R., Katahira, M., Chinenn, T., Tamura, H., Tamano, H., Takeda, A., 2022. Intracellular hydrogen peroxide produced by 6-hydroxydopamine is a trigger for nigral dopaminergic degeneration of rats via rapid influx of extracellular Zn2+. Neurotoxicology 89, 1–8. https://doi.org/10.1016/j.neuro.2021.12.006.
Oda, S., Fukami, T., Yokoi, T., Nakajima, M., 2015. A comprehensive review of UDP-glucuronosyltransferase and esterases for drug development. Drug Metab. Pharmacokinet. https://doi.org/10.1016/j.dmpk.2014.12.001.
Ono, K., Yamada, M., 2007. Vitamin A potently destabilizes preformed α-synuclein fibrils in vitro: implications for Lewy body diseases. Neurobiol. Dis. 25, 446–454. https://doi.org/10.1016/j.nbd.2006.10.010.
Ott, M., Gogvadze, V., Orrenius, S., Zhivotovsky, B., 2007. Mitochondria, oxidative stress and cell death. Apoptosis. https://doi.org/10.1007/s10495-007-0756-2.
Paradies, G., Paradies, V., De Benedictis, V., Ruggiero, F.M., Petrosillo, G., 2014. Functional role of cardiolipin in mitochondrial bioenergetics. Biochim. Biophys. Acta Bioenerg. https://doi.org/10.1016/j.bbabio.2013.10.006.
Passi, S., Maggio, F., Ricci, R., Cocchi, M., 2003. Prolonged administration of ubiquinone (CoQ10) and ubiquinol diacetate (CoQ10) to rats and guinea pigs. Prog. Nutr. 5, 6–15.
Perrier, A.L., Massoulié, J., Krejci, E., 2002. PRiMA: the membrane anchor of acetylcholinesterase in the brain. Neuron 33, 275–285. https://doi.org/10.1016/s0896-6273(01)00584-0.
Picca, A., Guerra, F., Calvani, R., Romano, R., Coelho-Júnior, H.J., Bucci, C., Marzetti, E., 2021. Mitochondrial dysfunction, protein misfolding and neuroinflammation in Parkinson's disease: roads to biomarker discovery. Biomolecules 11, 1508. https://doi.org/10.3390/biom11101508.
Pruccoli, L., Morroni, F., Sita, G., Hrelia, P., Tarozzi, A., 2020. Esculetin as a bifunctional antioxidant prevents and counteracts the oxidative stress and neuronal death induced by amyloid protein in sh-sy5y cells. Antioxidants 9, 1–16. https://doi.org/10.3390/antiox9060551.
Pruccoli, L., Balducci, M., Pagliarani, B., Tarozzi, A., 2024. Antioxidant and neuroprotective effects of fucoxanthin and its metabolite fucoxanthinol: a comparative in vitro study. Curr. Issues Mol. Biol. 46, 5984–5998. https://doi.org/10.3390/cimb46060357.
Raza, C., Anjum, R., Shakeel, N.A., 2019. Parkinson's disease: mechanisms, translational models and management strategies. Life Sci. https://doi.org/10.1016/j.lfs.2019.03.057.
Rocha, E.M., De Miranda, B., Sanders, L.H., 2018. Alpha-synuclein: pathology, mitochondrial dysfunction and neuroinflammation in Parkinson's disease. Neurobiol. Dis. https://doi.org/10.1016/j.nbd.2017.04.004.
Santulli, C., Brizi, C., Micucci, M., Del Genio, A., De Cristofaro, A., Bracco, F., Pepe, G.L., di Perna, I., Budriesi, R., Chiarini, A., Frosini, M., 2017. Castanea sativa mill. Bark extract protects U-373 MG cells and rat brain slices against ischemia and reperfusion injury. J. Cell. Biochem. 118, 839–850. https://doi.org/10.1002/jcb.25760.
Seet, R.C.S., Lim, E.C.H., Tan, J.J.H., Quek, A.M.L., Chow, A.W.L., Chong, W.L., Ng, M.P. E., Ong, C.N., Halliwell, B., 2014. Does high-dose coenzyme Q10 improve oxidative damage and clinical outcomes in Parkinson's disease? Antioxid. Redox Signal. https://doi.org/10.1089/ars.2013.5801.
Setoguchi, S., Hidaka, R., Nagata-Akaho, N., Watase, D., Koga, M., Matsunaga, K., Karube, Y., Takata, J., 2020a. Novel cationic prodrug of ubiquinol-10 enhances intestinal absorption via efficient formation of nanosized mixed-micelles with bile acid anions. Molecules 25. https://doi.org/10.3390/molecules25030546.
Setoguchi, S., Nagata-Akaho, N., Goto, S., Yamakawa, H., Watase, D., Terada, K., Koga, M., Matsunaga, K., Karube, Y., Takata, J., 2020b. Evaluation of photostability and phototoxicity of esterified derivatives of ubiquinol-10 and their application as prodrugs of reduced coenzyme Q10 for topical administration. BioFactors 46, 983–994. https://doi.org/10.1002/biof.1678.
Sharma, R., Bhate, L., Agrawal, Y., Aspatwar, A., 2025. Advanced nutraceutical approaches to Parkinson's disease: bridging nutrition and neuroprotection. Nutr. Neurosci. https://doi.org/10.1080/1028415X.2025.2469170.
Stiernagle, T., 2006. Maintenance of C. elegans. In: WormBook, pp. 1–11. https://doi.org/10.1895/wormbook.1.101.1.
Storch, A., 2007. Randomized, double-blind, placebo-controlled trial on symptomatic effects of coenzyme Q10 in Parkinson disease. Arch. Neurol. 64, 938. https://doi.org/10.1001/archneur.64.7.nct60005.
Su, L., Gao, K., Tian, Y., Xiao, X., Lu, C., Xu, J., Yan, X., 2024. Mitochondrial esterase activity measured at the single organelle level by nano-flow cytometry. Anal. Chem. 96, 810–820. https://doi.org/10.1021/acs.analchem.3c04321.
Suárez-Rivero, J.M., Pastor-Maldonado, C.J., Povea-Cabello, S., Álvarez-Córdoba, M., Villalón-García, I., Munuera-Cabeza, M., Suárez-Carrillo, A., Talaverón-Rey, M., Sánchez-Alcázar, J.A., 2021. Coenzyme q10 analogues: benefits and challenges for therapeutics. Antioxidants. https://doi.org/10.3390/antiox10020236.
Thirugnanam, T., Santhakumar, K., 2022. Chemically induced models of Parkinson's disease. In: Comparative Biochemistry and Physiology Part - C: Toxicology and Pharmacology. https://doi.org/10.1016/j.cbpc.2021.109213.
Turunen, Mikael, Appelkvist, E.-L., Sindelar, P., Dallner, G., 1999. Blood concentration of coenzyme Q10 increases in rats when esterified forms are administered. J. Nutr. 129, 2113–2118. https://doi.org/10.1093/jn/129.12.2113.
Umesh, M.C., Mukundan, G.K., Seekallu, S., 2023. Evaluation of pharmacokinetic parameters of ubiquinol acetate, ubiquinone and ubiquinol in male Sprague-Dawley rats – a comparative study. Indian J. Physiol. Pharmacol. 67, 191–196. https://doi.org/10.25259/IJPP_484_2022.
Ünal, İ., Çalışkan-Ak, E., Üstündağ, Ü.V., Ateş, P.S., Alturfan, A.A., Altinoz, M.A., Elmaci, I., Emekli-Alturfan, E., 2020. Neuroprotective effects of mitoquinone and oleandrin on Parkinson's disease model in zebrafish. Int. J. Neurosci. 130, 574–582. https://doi.org/10.1080/00207454.2019.1698567.
Venderova, K., Park, D.S., 2012. Programmed cell death in Parkinson's disease. Cold Spring Harb. Perspect. Med. 2, a009365. https://doi.org/10.1101/cshperspect.a009365.

Winkler-Stuck, K., Wiedemann, F.R., Wallesch, C.-W., Kunz, W.S., 2004. Effect of coenzyme Q10 on the mitochondrial function of skin fibroblasts from Parkinson patients. J. Neurol. Sci. 220, 41–48. https://doi.org/10.1016/j.jns.2004.02.003.

Wołosiak, R., Drużyńska, B., Derewiaka, D., Piecyk, M., Majewska, E., Ciecierska, M., Worobiej, E., Pakosz, P., 2021. Verification of the conditions for determination of antioxidant activity by ABTS and DPPH assays—a practical approach. Molecules 27, 50. https://doi.org/10.3390/molecules27010050.

Xu, Y., Li, K., Qin, W., Zhu, B., Zhou, Z., Shi, J., Wang, K., Hu, J., Fan, C., Li, D., 2015. Unraveling the role of hydrogen peroxide in α-synuclein aggregation using an ultrasensitive nanoplasmonic probe. Anal. Chem. 87, 1968–1973. https://doi.org/10.1021/ac5043895.

Yoritaka, A., Kawajiri, S., Yamamoto, Y., Nakahara, T., Ando, M., Hashimoto, K., Nagase, M., Saito, Y., Hattori, N., 2015. Randomized, double-blind, placebo-controlled pilot trial of reduced coenzyme Q10 for Parkinson's disease. Parkinsonism Relat. Disord. 21, 911–916. https://doi.org/10.1016/j.parkreldis.2015.05.022.

Yuhan, L., Khaleghi Ghadiri, M., Gorji, A., 2024. Impact of NQO1 dysregulation in CNS disorders. J. Transl. Med. 22, 4. https://doi.org/10.1186/s12967-023-04802-3.